STRENGTH AND DEFORMABILITY DISTRIBUTION IN UHPFRC PANELS

Cornelius OESTERLEE
PhD Student, Division of Maintenance and Safety (MCS), Ecole polytechnique fédérale de Lausanne (EPFL)

Emmanuel DENARIÉ
Senior researcher, Division of Maintenance and Safety (MCS), Ecole polytechnique fédérale de Lausanne (EPFL)

Eugen BRUEHWILER
Professor, Division of Maintenance and Safety (MCS), Ecole polytechnique fédérale de Lausanne (EPFL)

ABSTRACT:

The resistance as well as strain hardening and softening properties of UHPFRC depend on the type of matrix and mainly on the initial fibre dosage and final fibre distribution and orientation in the cast element. According to the final fibre distribution and orientation these properties may vary in a wide range.
The strength and deformability distribution in a thin UHPFRC panel is studied. Tensile and flexural specimens cut in different directions and at different positions in the panel are analysed in order to determine locally the mechanical material properties. The real fibre dosage, distribution and orientation are determined. The results show a wide scatter of the mechanical properties, whereas the physical properties, especially the air permeability, are not affected by the mechanical scatter.

Keywords: UHPFRC, fibre orientation, strain hardening, strength distribution, scatter of mechanical properties

1 INTRODUCTION

Ultra-High Performance Fibre-Reinforced Concrete (UHPFRC) provides high tensile strength with pronounced strain hardening and softening behaviour depending on the fibre dosage. Due to its dense matrix it has a very low permeability to aggressive substances. These properties allow applying UHPFRC successfully for the rehabilitation and reinforcement of existing structures, especially those exposed to high mechanical and chemical attack. A thin layer of UHPFRC added to an existing structural element increases the load bearing capacity, the serviceability and durability of the structure.
Two main aspects for this type of application are the material strength and its deformability. The deformability and viscoelastic properties are of particular importance. They allow the material to cope with restrained shrinkage and the degree of restraint given by the mechanical and geometric properties of the existing element.
Tensile strength and deformability depend on the type of matrix, the initial fibre dosage and the final fibre distribution and orientation in the cast element. Depending on the geometry of the element and the pouring sense the scatter in the mechanical properties can be very important. The mechanical behaviour may vary from no strain hardening at all to an increased deformability. The same applies for the tensile strength. It can reach values up to 17 MPa or in special cases be even lower than the matrix strength if uniformly oriented fibres parallel to the cracking plane weaken the section.
Material tests on individually cast specimen may not be representative and overestimating due to a repetitive, optimized fabrication process and the special specimen shape that may reduce the scatter and favour an aligned fibre orientation leading to high strength values.
The presented study is based on a full size structural element – a vertically cast panel in UHPFRC. It was cut into individual specimens for tensile and bending tests. The results show the scatter and the distribution of the material properties in the UHPFRC panel.

2 EXPERIMENTAL PROGRAM

2.1 Material and Specimens

The present study is based on a UHPFRC-type developed at EPFL-MCS, Switzerland with 3 % high strength straight steel fibres. CEM III type cement and silica fume are used for the matrix. The fibre aspect ratio is 81 and the water/cement-ratio 0.16. The fresh concrete provides an excellent workability and fills the

formwork without air bubbles and gives a very smooth surface finish.
The examined panel had an original size of 150·300 cm² and a thickness of 4.2 cm. It was poured vertically, the long edge standing up. The specimens for uniaxial tensile (label TxH/V) and 4-point bending (label FxH/V) tests were cut at different locations and in two orientations – vertically and horizontally – as shown in figure 3. In total 13 specimens were tested in tension and 12 in bending. Some tensile specimens were tested twice if the macro crack location of the first test allowed performing a second test. The panel was cut using regular concrete cutting equipment. In order to reduce effects of fibre orientation at the formwork boundaries 50 mm wide stripes along the relevant edges were cut and excluded from the testing program. The specimens were tested at an age of 150 days, after being stored at laboratory conditions.

2.2 Air permeability

Before the structural tests the air permeability of the panel was studied with a Torrent air permeability testing system [1, 2]. The system is based on the measurement of the pressure increase after an imposed vacuum in a defined period of time. A two vacuum-chamber setup with a circular main chamber in the centre and a surrounding secondary chamber reduces the effect of lateral air suction into the considered measurement volume.
32 measurements, 8 in the vertical sense and 4 in the horizontal sense arranged in a regular grid of 33·30 cm² were taken. The results show no preferential distribution of the kT-values. Obviously the quality of the matrix is randomly distributed within the panel, especially no gradient over the height can be observed. The geometric mean value of kT equals $0.0046 \cdot 10^{-16}$ m^2, which is representative for the lowest permeability class and by a factor of about 10 lower than best quality traditional concrete. Figure 1 shows the distribution of kT along four vertical traces with a spacing of 30 cm mapping the panel surface.

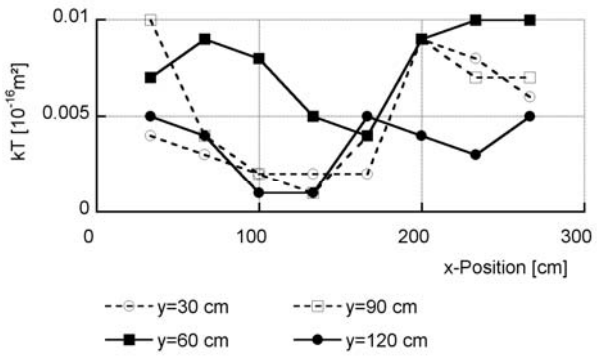

Figure 1: Air permeability kT, distribution along the vertical axis of the panel

In the serviceability state of a structural element it is the matrix permeability and microcracking that defines the protective function of the UHPFRC-layer in the above described field of application as (protective and waterproofing) coating for rehabilitation and strengthening purposes.

2.3 Test setup – tensile tests

The 100 cm long and 20 cm wide tensile specimens cut from the panel were tested in a 1000 kN servo-hydraulic testing machine in displacement controlled mode. The specimens were fastened in the machine with laterally acting, hydraulic clamping jaws. To prevent cracking in the clamping zone the ends of the specimens were reinforced with epoxy-glued on aluminium plates with a size of 2·250·200 mm³. The central 500 mm long part of the specimens was instrumented with two laterally mounted LVDTs for the measurement of the overall elongation and 5 strain gauges, measuring over a length of 100 mm each, for the local deformation. The loading rate was set to 0.02 mm/min in the pre-peak domain and 0.2 mm/min in the post-peak domain. The measurements were recorded at a frequency of 2 Hz.

2.4 Test setup – bending tests

The 50 cm long and 20 cm wide specimens for bending were tested in a 200 kN servohydraulic, displacement controlled testing machine with a static system as shown in figure 2. The midspan deflection was measured by two LVDTs at the edge of specimen. The loading rate was set to 0.02 mm/min pre-peak and 0.2 mm/min post-peak.

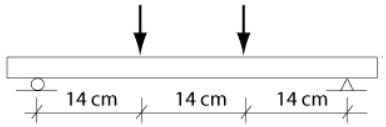

Figure 2: 4-point bending test setup

3 EXPERIMENTAL RESULTS

3.1 Results of tensile tests

The results of the tensile tests were obtained from five zones defined by the individuel specimen orientation and location in the panel (figure 3). The major gray arrow indicates the direction of casting (left picture), the gray arrows on the right indicate the predominant fibre orientation estimated based on the coefficient of orientation and the tensile strengths. The long edge of the panel is defined as x-axis, the short as y-axis.

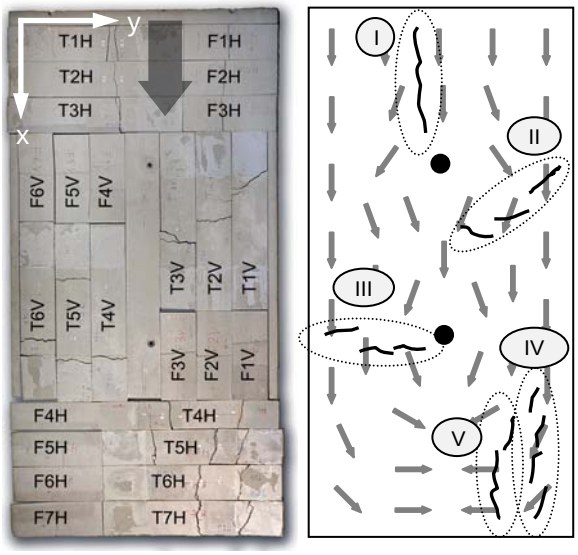

Figure 3: Definition of zones I to V, cracking and predominant fibre orientation

Zone I, specimens T1H, T2H, T3H, horizontal: located at the top of the element. The specimens provide a maximum strength that is significantly lower than the pure matrix strength (figure 4). In this case the fibres predominantly oriented parallel to the loading direction reduce the matrix strength and interact as local defects. The vertical fibre flow into the formwork is basically maintained in the top 60 cm of the element
There are two possible approaches to explain the reduced tensile strength in the top area of the panel:

a) A simplified linear elastic fracture mechanics approach interprets the effect of parallel fibres as multiple defects. Assuming the specific specimen to be an infinite plate and the fibres oriented perpendicular to the main stress field to be circular or elliptic defects the stress at the edge of the defect increases at least by a factor of 3 and thus reduces the maximum strength of the specimen.

$$\sigma_{max} = \sigma_0 \cdot (1+2 \cdot a/b) \qquad (2)$$

where,

σ_0 : uniform stress applied to the element
a, b: semi-major and semi-minor axis of an the ellipse

b) Estimating 50 % of the fibre length being oriented parallel to the cracking plane and multiplying by the number of fibres per unit area the projected fibre surface, this represents approximatly 30 % of the cross section, reducing thus the effective residual cross section to 70 %.

A combination of these two effects may cause the locally significantly lower tensile strength compared to the rest of the panel. At the same time there is a pronounced softening branch due to the pull out work by the effective fibres but at a low strength level.

Zone II, specimens T1V, T2V, T3V, vertical: located 100 cm below the formwork opening: the fibre orientation is influenced by the vicinity of the centrally placed formwork tie that crosses the formwork deviating the fibre flow. The resistance of this series of specimens is slightly above the pure matrix strength and shows more of a plastic plateau than real strain hardening behaviour (figure 5).

Zone III, specimens T4V, T5V, T6V, vertical: located 200 cm below the formwork opening: the fibre orientation here seems to be more favourable for the chosen testing direction. The results are significantly above the results of the zone II specimens. The average tensile strength is 12.9 MPa and all specimens show a distinct strain hardening behaviour with a deformation of 3 ‰ at peak strength, respectively 5.4 ‰ for specimen T4V (figure 6).

Zone IV, specimens T4H, T5H-1, T6H-1, T7H-1, horizontal: located at the lower right corner, first test run. These specimens were tested twice due to the location of the rupture in the first test run. The first test results resist an average maximum strength of 10.4 MPa with a mixed response in deformability. Some specimens reach up to 2.4 ‰ whereas others do not exceed 0.5 ‰. The fracture zone is located in an area where the flow of the fresh concrete is influenced and guided by the formwork boundaries, forcing the fibres from a more vertical into a more horizontal orientation at the bottom of the element (figure 7).

Zone V, specimens T5H-3, T6H-2, T7H-2, horizontal: located at the lower part of the panel, left of zone IV. These results are obtained from the same specimens as in zone IV but in a second test run. Therefore they are predamaged which is indicated by the slightly lower stiffness in the elastic domain. Now the fracture zone is located more to the centre of the panel, where the fibre orientation is mainly influenced by the near presence of the lower formwork boundary. Fibres are oriented in a more horizontal way. The average strength for this series is 15.5 MPa, which represents the highest strength values found in the whole panel. The coefficient of orientation determined in specimen T6H-2 confirms the expected predominantly horizontal fibre orientation. All specimens provide strain hardening up to 3.4 ‰ (figure 8).

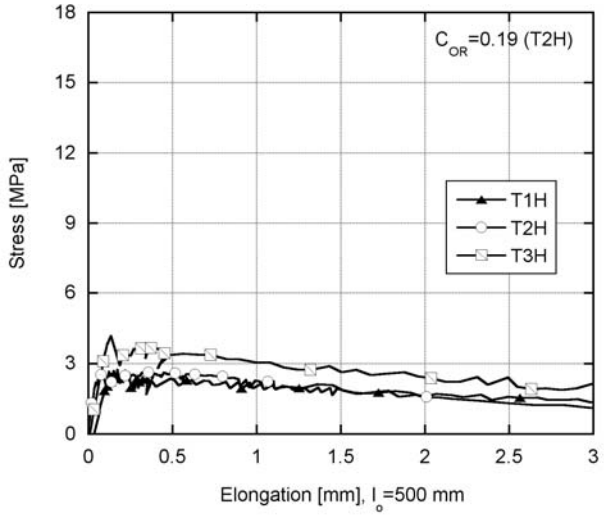

Figure 4: Tensile tests zone I (T1H, T2H, T3H)

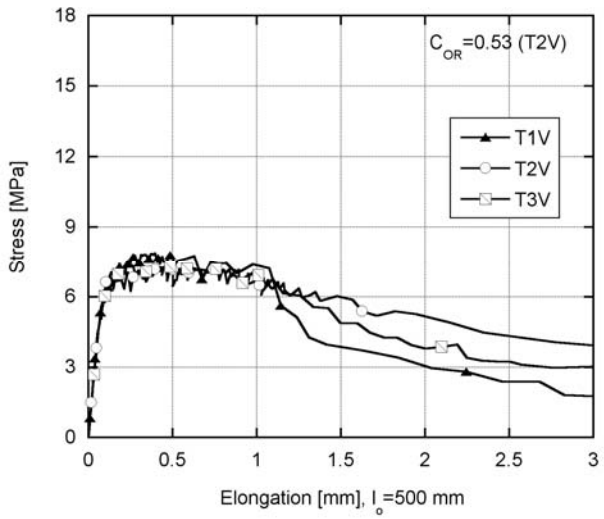

Figure 5: Tensile tests zone II (T1V, T2V, T3V)

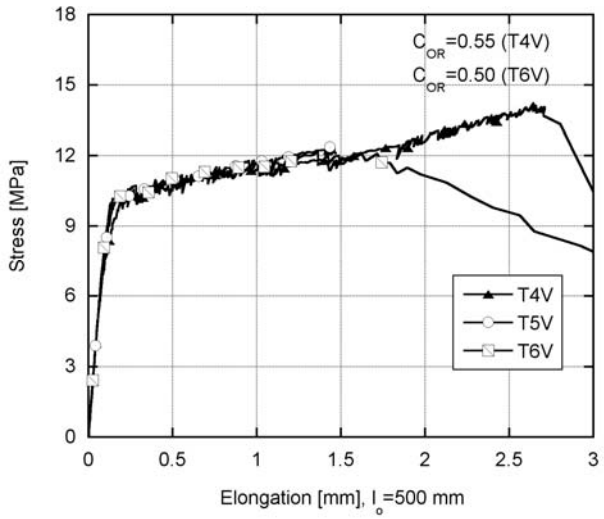

Figure 6: Tensile tests zone III (T4V, T5V, T6V)

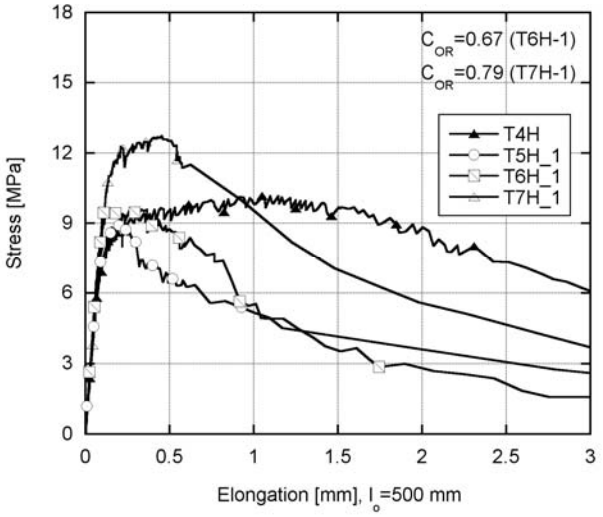

Figure 7: Tensile tests zone IV (T4H, T5H-1, T6H-1, T7H-1)

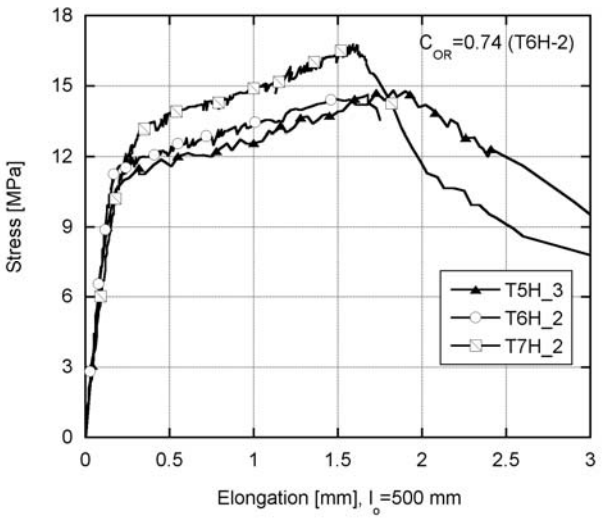

Figure 8: Tensile tests zone V (T5H-3, T6H-2, T7H-2)

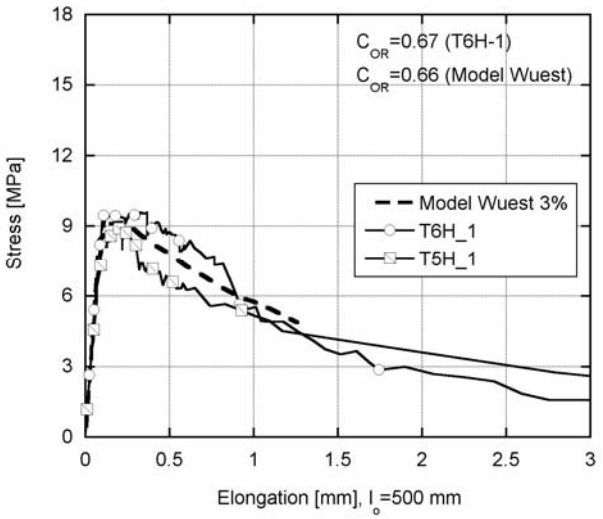

Figure 9: Tensile tests, comparison model Wuest [3] and T6H-1, same C_{OR}

The tensile response of the investigated type of UHPFRC was analytically predicted by Wuest [3] for a mix with 3 % fibres and a coefficient of orientation C_{OR}=0.66. The same coefficient of orientation was experimentally found in zone IV, namely in specimen T6H-1. As shown in figure 9, the experimental tensile response corresponds very well to the predicted response by Wuest.

The above presented results show the wide scatter in maximum strength and deformability observed in the five zones of the analysed panel. Obviously the macrocrack paths cross the chosen specimen boundaries. The macrocracks follow the weakest plane in the specific zone, independent on the actual specimen size and shape. The small scatter within the different zones, except for zone IV, confirms the above observation. The average maximum strength yields to 9.8 MPa with a standard deviation of 4.1 MPa. The frequency distribution of the maximum strength $f_{t,u}$ is shown in figure 10.

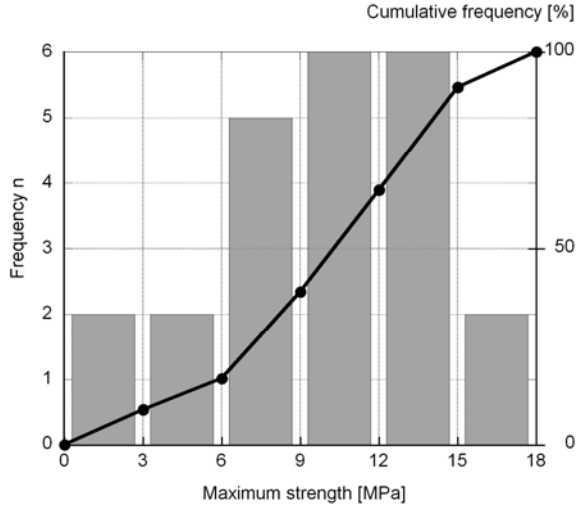

Figure 10: Frequency distribution of $f_{t,u}$

Regarding the geometric strength distribution in the panel it can be observed that the maximum tensile strength σ_{max} increases from locations at the top of the element to the bottom for both types of specimens, horizontally and vertically cut. Figure 11 and figure 12 show the mapping of the results along the vertical axis for the horizontally cut and tested specimens as well as along the horizontal axis for the vertically cut and tested specimens. As will be shown in paragraph 3.3, the fibre distribution being homogenous, the increase of strength is closely related to the fibre orientation.

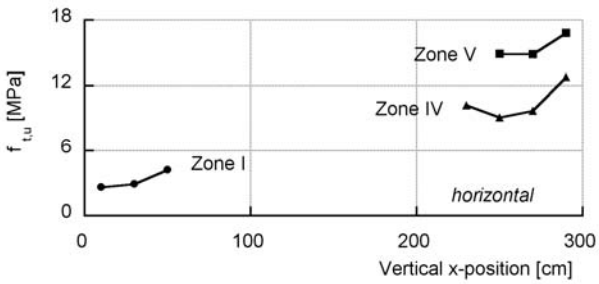

Figure 11: Mapping of $f_{t,u}$ horizontally oriented specimens

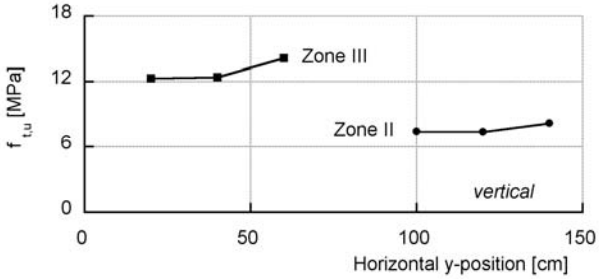

Figure 12: Mapping of $f_{t,u}$ vertically oriented specimens

3.2 Results of bending tests

The results of the bending tests are less pronounced with a higher scatter regarding the regional grouping of the results. The comparison between tensile and bending tests is somehow difficult since the specimens are obviously not taken from the exact same region. In addition the results in bending depend more on the mode of failure, namely if one or two macrocracks open.

In general the trend observed in direct tension is confirmed as the different regions show qualitatively the same tendency as the tensile tests. Especially specimen F1H, corresponding to T1H shows the influence of parallel oriented fibres. Bending results obtained from zone III have the same low scatter than most of the direct tension tests.

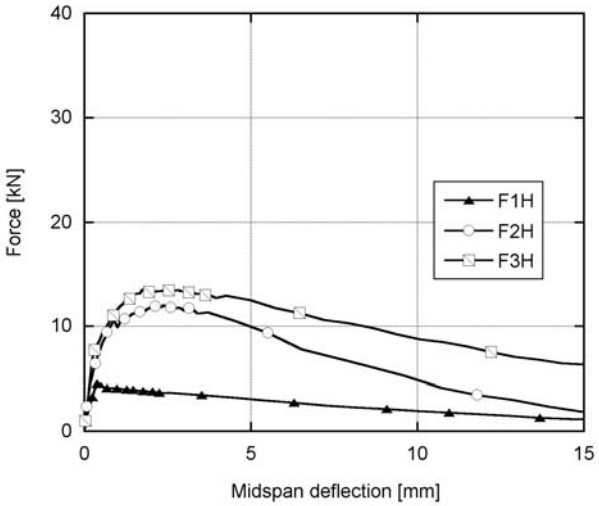

Figure 13: Bending results zone I

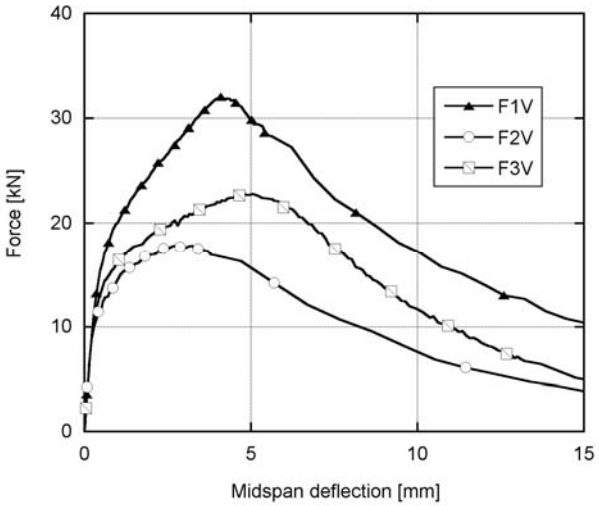

Figure 14: Bending results zone II

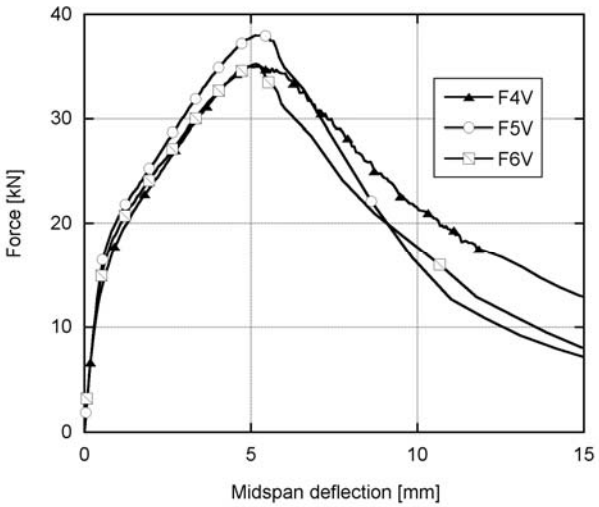

Figure 15: Bending results zone III

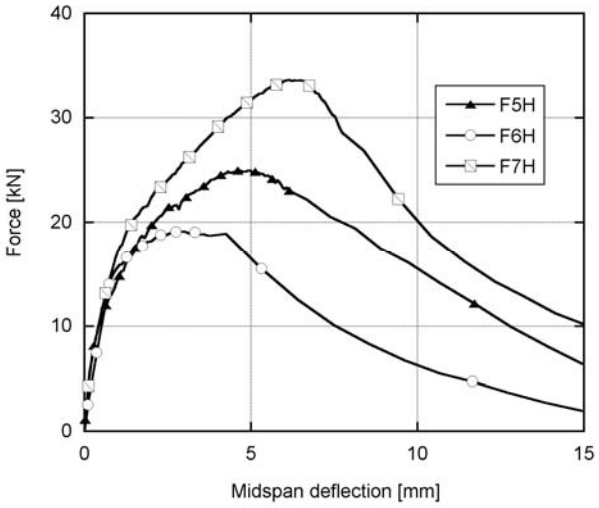

Figure 16: Bending results zone IV

3.3 Fibre distribution and orientation

In order to determine the spatial orientation of the fibres, cubes of 3·3·3 cm³ were cut from the ruptured tensile specimens as close as possible to the fracture zone. Two surfaces, one parallel and one perpendicular to the direction of loading, were prepared and polished in order to remove cutting traces and residues from the surface. The surface was then scanned area by area with a Scanning Electron Microscope (SEM) at a resolution of 10 microns. The images were then assembled and analysed with a fibre counting software application.
In addition the real fibre dosage was determined by crushing adjacent UHPFRC cubes, separating fibres from the crushed matrix and weighting them. Except for two specimens (T4V: 2.8 %; T6V: 4.1 %) the variability of the fibre distribution was found to be very little given an average of 3.08 % and a standard deviation of 0.08 % compared to a theoretical dosage of 3%. This means that even for the important fill-in height of 300 cm no significant fibre segregation occurred. The main source of the scatter of the mechanical response is thus the anisotropic fibre orientation.

Figure 17 shows the polished surfaces of a specimen located very close to the top of the panel (T2H). The number of fibres found in the two adjacent surfaces is very different and varies form 29 fibres/cm² in one direction to 123 fibres/cm² in the perpendicular direction. The results of the tensile test clearly show the influence of the extreme anisotropic fibre distribution. The section with the low number of fibres resists only 2.9 MPa in direct tension.

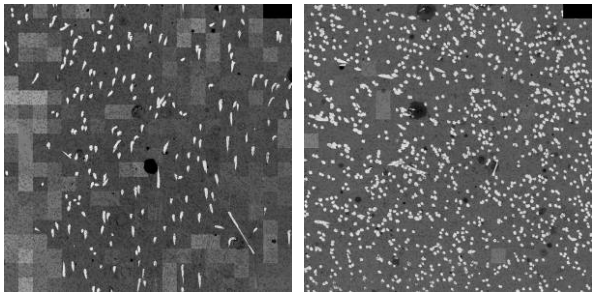

Figure 17: Fibre count on a surface parallel and perpendicular to the macrocrack, specimen T2H, non-uniform fibre orientation

Figure 18 shows two surfaces of a specimen located in the centre of the panel (T2V). Here the fibre distribution is more homogeneous and the number of fibres/cm² is 83 and 100 respectively.

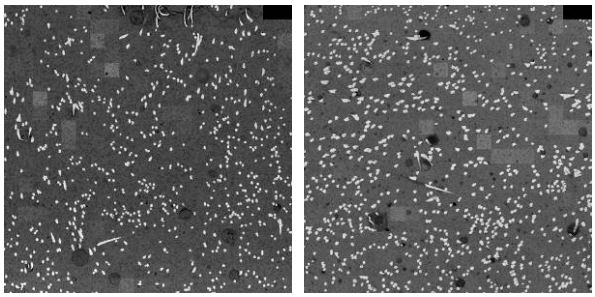

Figure 18: Random fibre orientation in perpendicular cuts in specimen T2V

With the results of the image analysis the coefficient of

orientation C_{OR} is determined using equation (1):

$$\mu = N_f \cdot A_f / V_f \quad (1)$$

where,

N_f : number of fibres per unit area
V_f : total volume of fibres
A_f : section of a fibre.

The maximum tensile strength is related to the coefficient of orientation (figure 19). The strength values for C_{OR}=0 and C_{OR}=1 were estimated based on the work of Wuest [3]. C_{OR}=0 corresponds to the plain matrix strength. The others values follow a trend, where the pure matrix strength defines the lower boundary and the fibre efficiency increases non-linearly with an increasing coefficient of orientation. The results for T4V and T6V somehow don't follow that trend. This can be explained due to a locally increased fibre dosage (T6V: 4.1 % instead of 3 % according to the recipe). The results of the specimens perpendicular to the initial loading direction are labeled * and plotted with the same shape as the original specimens but without fill. The results of the these specimens confirm very well the observed trend.

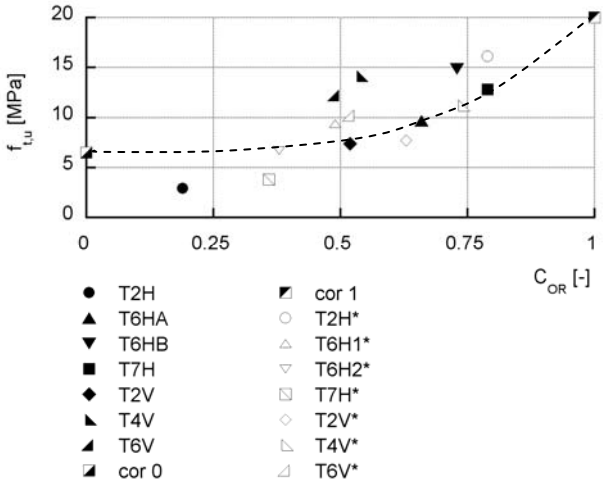

Figure 19: Maximum strength over C_{OR}

Table 1 summarises the results of the direct tension tests and the fibre distribution and orientation.

Table 1: Mechanical and fibre properties of tensile specimens

ID	V_f [%]	$N_f \parallel$ [1/cm²]	$N_f \perp$ [1/cm²]	$C_{OR} \parallel$ [-]	$C_{OR} \perp$ [-]	$f_{t,u}$ [MPa]
T1H						2.6
T2H	3.14	29.1	123.3	0.19	0.79	2.9
*T2H**						*16.1*
T3H						4.2
T4H						10.2
T5H-1						9.1
T5H-3						14.9
T6H-1	3.07	101.1	74.9	0.67	0.49	9.7
*T6H*1*						*9.4*
T6H-2	2.96	108.5	56.7	0.74	0.39	14.9
*T6H*2*						*6.7*
T7H-1	3.07	121.4	55.4	0.79	0.36	12.8
*T7H**						*3.8*
T7H-2						16.8
T1V						8.2
T2V	3.17	83.2	100.1	0.53	0.63	7.4
*T2V**						*7.7*
T3V						7.4
T4V	2.76	74.9	102.5	0.55	0.75	14.1
*T4V**						*11.2*
T5V						12.4
T6V	4.13	101.7	107.8	0.50	0.53	12.2
*T6V**						*10.2*
	Ø 3.2					Ø 9.8
	σ 0.4					σ 4.1

*these specimens were cut from the initial specimen and tested perpendicular to the initial loading direction, dimension 200·42·50 mm³
$\parallel$ parallel to the initial cracking plane
$\perp$ perpendicular to the inital cracking plane

4 STRUCTURAL CONSIDERATIONS

Uniaxial tensile tests reveal directly the capacity and weakness of UHPFRC. At the same time they are not necessarily representative for structural applications of UHPFRC. Only in a few cases the uniaxial tensile strength is directly addressed. Especially in the above mentioned field of application for rehabilitation and reinforcing purposes there is an interaction between the UHPFRC layer and the existing structure. The material is stressed in a mixed mode combining bending and tension. Whereas the experimentally found tensile responses are valid only locally, in a full scale structure depending on the loading scheme there will be local redistribution of internal forces as it is typical for hyperstatic structural elements and systems. Considering this, a locally identified low strength area does not necessarily affect the overall structural response in the same intensity as the low tensile strength values may suggest.
Therefore the wide scatter found in the analysed panel can be taken exemplary for the property distribution in a full scale structural element but does not allow a direct conclusion on the structural behaviour of the panel as a whole or a similar structural element. The panel as whole will respond in a more uniform way.
Yet, the definition of characteristic design values based on a test series as the one presented here is not obvious. Applying the typical approach choosing the 5 % fractile would be very penalising for UHPFRC. In fact it would reduce the very high average tensile strength to a level in the same order of magnitude as ordinary concrete. Important advantages of UHPFRC would be given up this way and its mechanical and also economic efficiency be questioned.

5 CODES AND RECOMMENDATIONS

In codes and recommendations the issue of fibre

distribution and orientation is encountered with correction factors that count for such inhomogeneities. In general it is recommended to produce representative specimens and to test them locally at varying orientations and locations in order to determine strength values that are close to the intended application. The French guidelines recommend to apply a K-factor of 1.25 for loads on a structural level and K=1.75 for local loads [4]. The German state of the art report identifies the issue but doesn't give a specific recommendation how to deal with it [5]. The Japanese recommendations [6] use an approach based on inverse analysis of the flexural strength and a material safety factor.
Finally there exists still no comprehensive and conclusive concept to determine characteristic values for material properties and safety factors for the application of UHPFRC, another difficulty being also the vast number of different recipes and material classes available worldwide.

6 CONCLUSIONS

The presented study shows the capacity of UHPFRC with 3 % fibres. The material combines excellent workability with strain hardening in tension. The conducted test series based on a structural element cast in a very unfavourable way revealed and quantified the wide scatter of the mechanical properties but also confirmed a very high average tensile strength as well as deformability (strain hardening). The material properties were identified with a high number of uniaxial tensile tests, that directly show strength and deformation capacity and their distribution. The mechanical properties were classified in zones and related to the real fibre orientation and distribution, determined by fibre counting in cross sections parallel and perpendicular to the loading direction.

(1) The strength in the panel varies mainly from the top to the bottom along the casting direction of the panel.
(2) The experimentally determined coefficient of orientation confirms the results of the tensile tests and allows to estimate the predominant fibre orientation in the whole panel. The local fibre distribution is uniform and shows low scatter. No signs of segregation could be found.
(3) The permeability, determined by means of air permeability testing, is independent on the distribution of the mechanical properties. It is randomly distributed.
(4) Tensile strength values below the pure matrix strength can be explained by a reduced net cross section due to fibres oriented parallel to the cracking plane and stress concentrations around fibres seen as local defects.
(5) Within the variety of tensile response found in the different regions of the panel there are some that agree very well with an analytical approach to predict the tensile response. Though other tensile responses fall below or exceed by far the analytically predicted ones.

The obtained results can be used as basis to optimize the geometry and number of specimens for a reliable material characterisation.
In general the structural response of an element such as presented above will be less influenced by the extreme values but mainly by the average strength, depending on the character of loading – global or local.

ACKNOWLEDGEMENT

The authors would like to express their sincere gratitude to CTI (Commission of Technology and Innovation) and Cemsuisse for funding of this research project.

REFERENCES

1. Denarié E., Maître M., Conciatori D., Brühwiler E., "Air permeability measurements for the assessment of the in situ permeability of cover concrete", Proceedings, International Conference on Concrete Repair, Rehabilitation and Retrofitting (ICCRRR 2005), 21-23, November 2005, Cape Town, South Africa
2. Torrent R., "A two-chamber vacuum cell for measuring the coefficient of permeability to air of the concrete cover on site", Materials and Structures, Vol. 25, No. 150, 1992, pp 358-365.
3. Wuest, J., "Comportement structural des bétons de fibres ultra performants en traction dans des éléments composés", Thèse EPFL, 2007
4. Association Francaise de Génie Civil, "Ultra High Performance Fibre-Reinforced Concretes", 2002
5. Deutscher Ausschuss für Stahlbeton, "Sachstandsbericht Ultrahochfester Beton", Heft 561, 2008
6. Japan Society of Civil Engineers, "Recommendations for design and construction of ultra high strength fibre reinforced concrete structures (Draft)", 2006